

Stress Relaxation and Creep of 12 to 35 μm Copper Foil

H.D. MERCHANT

Gould Electronics, Eastlake, OH 44095

Stress relaxation and creep of the electrodeposited and rolled copper foils, 12–35 μm thick, are investigated near yield stress and near room temperature. The stress relaxation does not obey a logarithmic time law; the creep appears to follow a power function. These deviations from the expected logarithmic behavior are thought to be caused by very small grain size, unstable non-equilibrium defect structure and extensive micropore population (vacancies and vacancy clusters) typical of the electrodeposit. Relaxation and creep are significantly lower for the rolled (than for the electrodeposited) foil. Decreasing the electrodeposit thickness has an effect of enhancing relaxation and creep, attributable to a limited nucleation on the cathode surface and consequent generation of microvoids between growth clusters in the vicinity of the substrate. The foil thickness effect on creep and stress relaxation is not observed for the rolled foil, which is prone to embrittlement and stiffening at about 323K.

Key words: Copper, creep, electrodeposit, foil, stress relaxation

INTRODUCTION

Limited attention has been paid to the intrinsic uniaxial stress relaxation¹ and creep^{1–3} of the free-standing electrodeposited polycrystalline copper film or foil. For short durations (less than 60 min) near room temperature, the creep at stresses below the yield stress is often logarithmic with time and exponential with stress;^{2–3} however, the logarithmic character is lost for longer times or higher stresses or temperatures. Likewise, the stress relaxation above room temperature appears logarithmic only for relatively short time segments.¹ The intrinsic stress relaxation of the free-standing vapor deposited copper film has not been examined; however, the creep of vapor deposited film or foil obeys the logarithmic⁴ or power⁵ time functions, the former for short durations and for relatively low temperatures and stresses.

The stresses introduced during deposition and processing, as well as those created during service by

temperature excursions, may reach high levels due to thermal expansion difference between deposit (film/foil) and substrate. The long term creep or cumulative relaxation (ratcheting), with ultimate stress-rupture failure, becomes a serious reliability hazard. Furthermore, it is recognized that the mechanical properties of thin films or foils tend to differ greatly from those of bulk materials of identical composition.^{6,7} This unique mechanical response of film or foil derives from its very fine-scaled microstructure and non-equilibrium defect structure,⁸ which is highly unstable during mechanical or thermal stimulus. The concentration of lattice defects (dislocations, twins and point or volume defects) can be very high; in particular, vacancies, micropores or vacancy-impurity complexes can facilitate or hinder the deformation process. The presence of a large number of excess vacancies and submicropores even at temperatures $\sim 0.2 T_m$ may give rise to mechanisms which occur in bulk metals only at temperatures $> 0.5 T_m$ (T_m = melting temperature).⁸ The dislocations, which reside primarily in substructural configurations,⁹ may be acti-

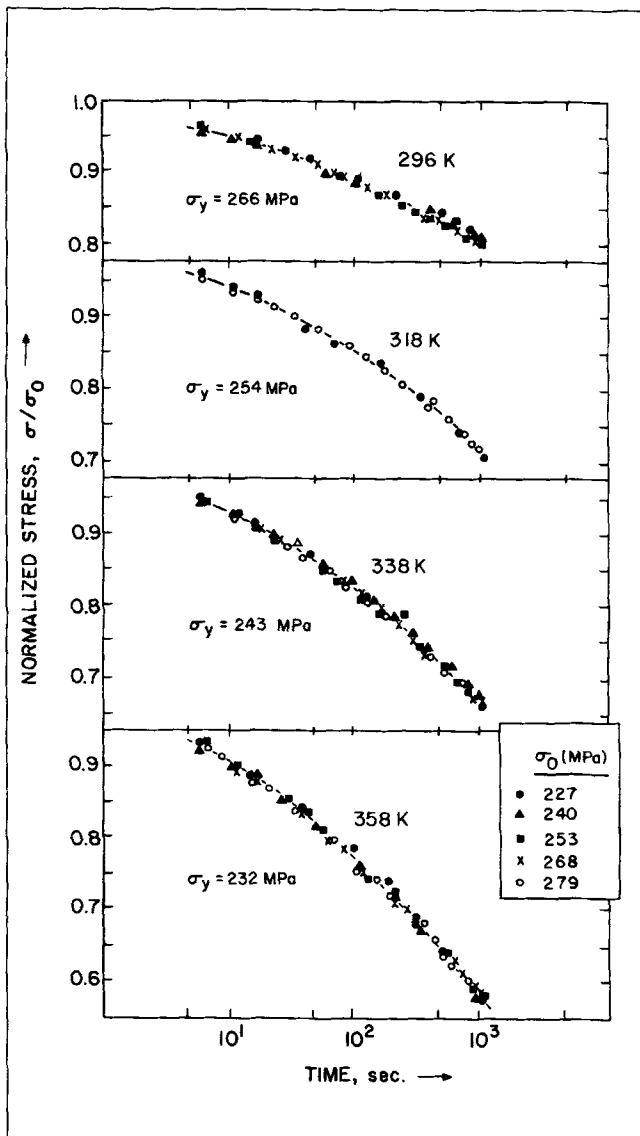


Fig. 1. Stress relaxation of 35 μm thick electrodeposit in terms of normalized stress.

ated at stresses considerably below the macroscopic flow stress.⁸

Several attempts have been made to calculate the thermal activation parameters during uniaxial creep of copper films and foils,^{5-8,10-13} but none during stress relaxation. The differential temperature and differential stress type experiments (to ensure structural constancy) to determine the activation parameters are planned for the future; the goal of this investigation, however, is to establish the preliminary temperature, stress and time dependency of creep and stress relaxation near or slightly above room temperature and yield stress. The structural changes during creep and relaxation are especially difficult to characterize for the films due to extremely fine scale of the microstructure; these too will be investigated in the future. Instead, the difference in mechanical response of the rolled vs deposited foils, identically dimensioned, is attempted in this study to establish the unique character of deposited metals.

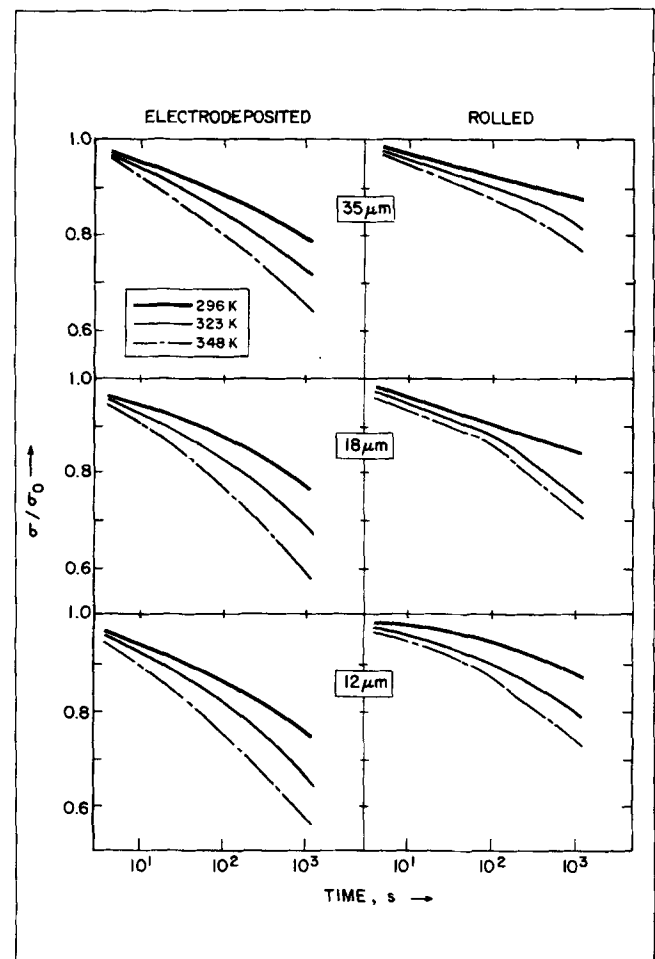


Fig. 2. Stress relaxation curves for 12, 18, and 35 μm thick electrodeposited and rolled foils (σ_0 near σ_y ; for σ_y values, see Fig. 8).

EXPERIMENTAL

The electrodeposited (ED) and rolled (R) copper foils, nominally 12, 18, and 35 μm thick, were utilized. The 4N purity electrodeposited foils were produced on a commercial roll plater, from the additive-free acidified copper sulfate solution, at moderate overpotential. The roll speed was adjusted to deposit a required thickness on a chromium substrate; the deposit was continuously stripped on to a receiving roll at a constant speed. A 12" thick electrolytic tough pitch (ETP) copper ingot was thermomechanically processed on a commercial roll/anneal facility to the required foil thickness in hard temper (heavy reduction cold-rolled condition). Prior to the stress relaxation or creep tests, the foils were stabilized at 358K for one hour.

The foil microstructure and defect structure were characterized by transmission electron microscopy (TEM) and x-ray diffraction Fourier line analysis (XRD/FLA), respectively; the line broadening providing estimates of dislocation density and "particle" size, and the line asymmetry providing estimate of twin spacing.¹⁴ The ED foils displayed an equiaxed grain structure, the average mid-thickness planar view grain size varying from about 0.28 μm for the 12

μm foil to 0.40 μm for the 35 μm foil. No substructural details were discernible in TEM even at very high magnifications. The R foil displayed a highly pancaked grain structure, the grain boundaries stretched out in the rolling direction; typically, five to ten grains, pancaked between the foil surfaces, were observed. The grain size anisotropy in the R foil is apparently due to (i) rolling and (ii) constraint provided by foil surfaces during the inter-pass recrystallization anneal. A dislocation cell structure, again elongated in the rolling direction, was observed. Typical dislocation density for either foil type was about 10^{11} cm^{-2} ; the foils were free from (growth or deformation) twins or stacking faults. The substructure, particle or cell size, was an order of magnitude smaller than the grain size. The stabilization anneal (358K, one hour) had no discernible effect on the grain structure or the substructure.

The mechanical tests were performed on the computer-based Sintech system; the equipment and the test sample dimensions have been described elsewhere.¹⁵ The samples were cut transverse to the substrate markings (ED foil) or rolling direction (R foil). The sample was loaded to or near the yield load

at $5 \times 10^{-4} \text{ s}^{-1}$ strain rate. The strain monitoring by crosshead movement and the small sample thickness resulted in

- Low apparent elastic modulus (a slight bending of the elastic portion of the stress/strain curve),
- Gradual yield transition, and
- Somewhat imprecise definition of yield level, especially the yield strain characterization.

However, this did not alter the validity of the relaxation or creep results. The stress relaxation and creep tests were conducted by monitoring the crosshead displacement, through an appropriate feedback software, to within $\pm 5 \times 10^{-5}$ strain. For the stress relaxation test, the crosshead motion was arrested and the relaxation was recorded continuously for about 1200 s, the total relaxation not exceeding 50%. For the creep test, the load was held stationary and the strain was recorded continuously for about 1800 s, the total strain not exceeding 5%. The initial load for the relaxation test and constant load for the creep test were varied between 0.80 and 1.30 of the yield load. The tests were isothermal, the test temperatures between 296 and 358K were utilized.

RESULTS

Typical stress relaxation results on semi-logarithmic plots were nonlinear (on a semi-log scale), consistent with the only available previous data,¹ suggesting significant changes in microstructure or defect structure with the relaxation time. The curves

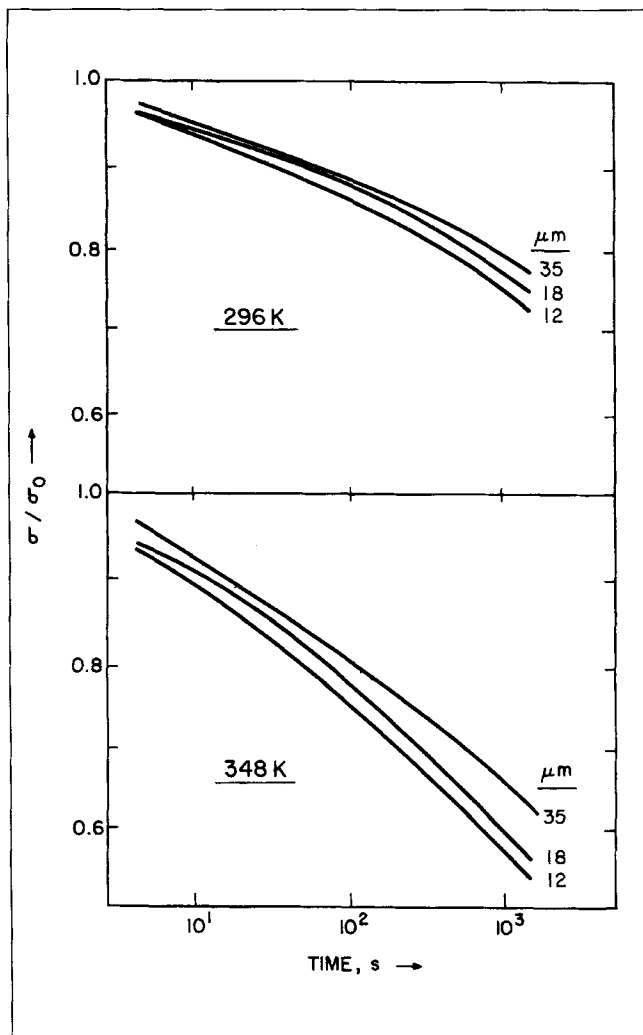


Fig. 3. Effect of thickness of electrodeposited foil on stress relaxation.

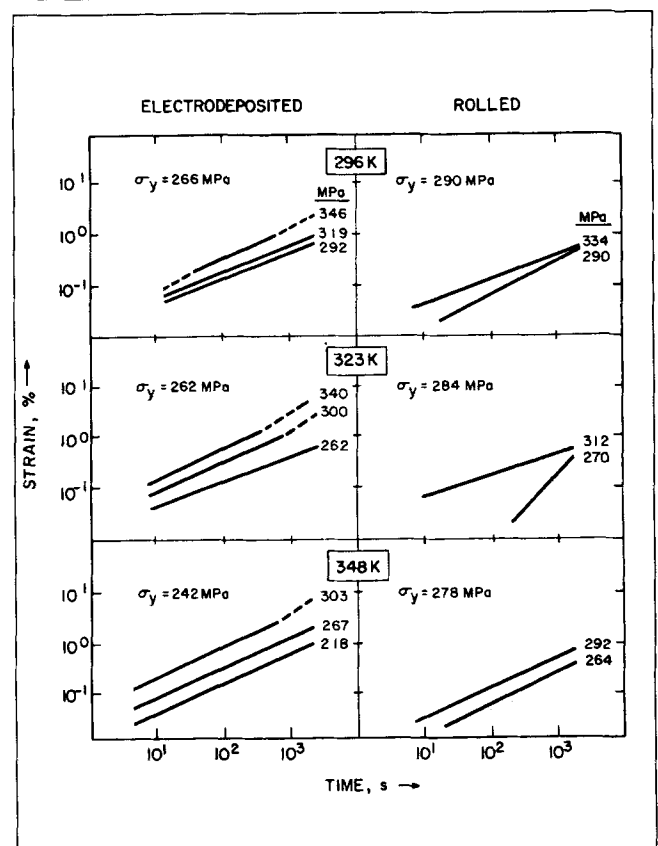


Fig. 4. Creep curves for 35 μm thick electrodeposited and rolled foils.

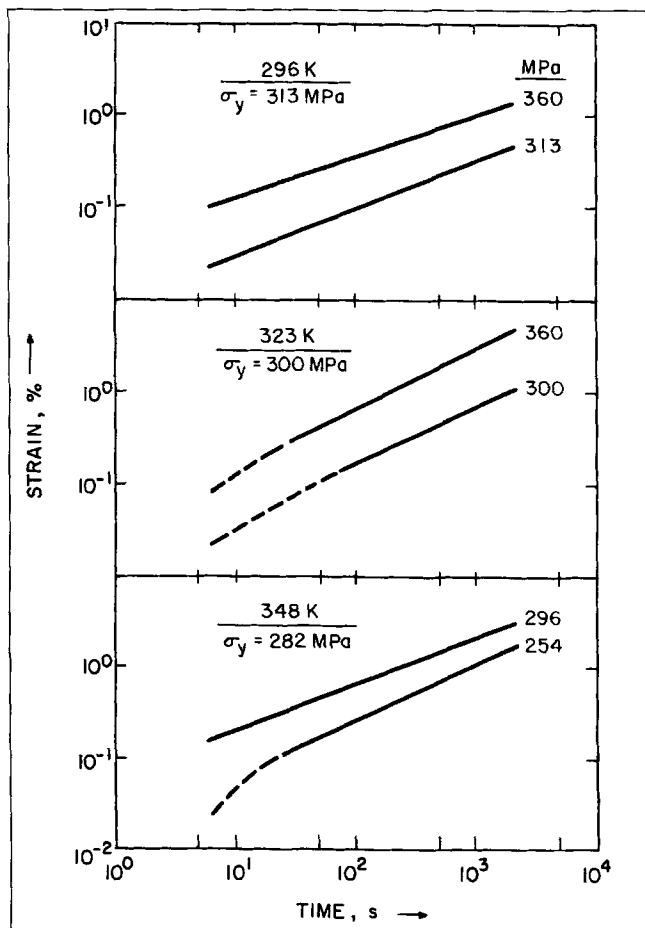


Fig. 5. Creep curves for 18 μm thick electrodeposited foil.

for varying initial stress (σ_0) were approximately parallel, indicating a possible vertical or horizontal shift to generate a master curve for each temperature. The stress normalized with respect to the initial stress (σ/σ_0) generated the master curve with relatively small data scatter, typical results for the 35 μm ED foil are shown in Fig. 1. The effects of temperature and foil thickness on the normalized stress relaxation for the ED and R foils are summarized in Fig. 2. Except for the 18 and 35 μm foils at 296K, the relaxation curves are not linear on the semi-log plots; in some tests, a sudden break in the linear portion of the plot is observed after a critical time (see 18 μm R foil at 323 and 348K), again suggesting microstructural factors which may abruptly accelerate the relaxation rate. For a given test temperature and foil thickness, the relaxation is greater for the ED foil (than for the R foil). Decreasing the foil thickness increases relaxation, this is especially true for the ED foil as illustrated in Fig. 3; further, the foil thickness effect is greater at the higher temperature. The relaxation rate and the extent of relaxation for the 12 μm ED foil are quite high, much higher than those for the R foil.

An apparent primary and steady-state creep behavior on closer examination obeyed a logarithmic time law below σ_y , but deviated from the logarithmic behavior at a critical time which decreased with

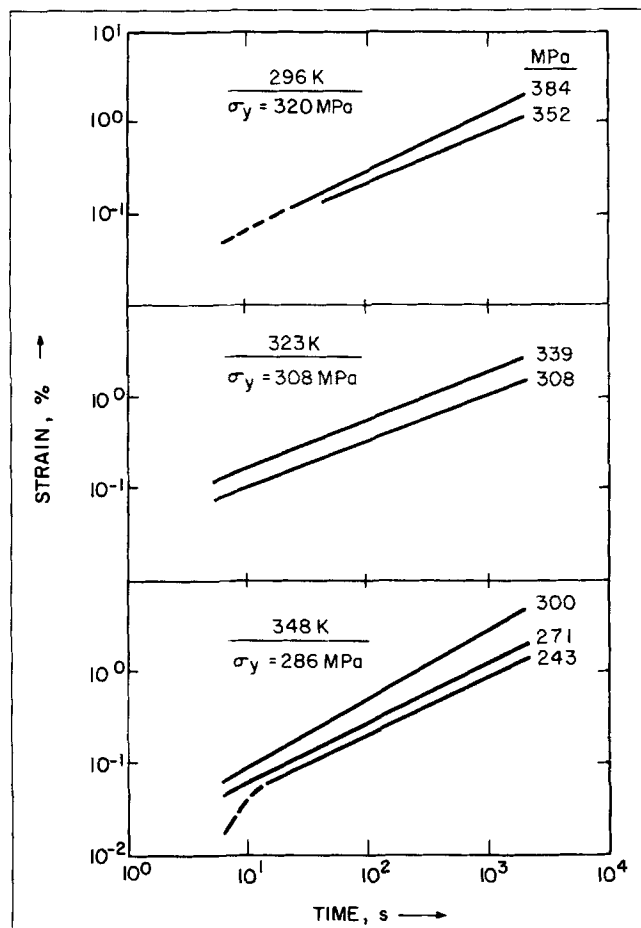


Fig. 6. Creep curves for 12 μm thick electrodeposited foil.

increasing stress. Below as well as above σ_y , the power law described the creep data more accurately until runaway creep (perhaps due to sample necking) ensued. Continuing creep strain in the runaway regime eventually resulted in failure by creep rupture. Logarithmic time dependence of creep for the electrolytic^{2,3} and vapor⁴ deposits and the parabolic time dependence for the vapor deposits⁵ have been observed before. The creep results for the 35 μm ED and R foils, plotted on a log-log scale, are shown in Fig. 4. The deviation from linearity, due to logarithmic behavior for short times and runaway creep for long times, are indicated as dotted portions of the plots. For a given set of stress and temperature conditions, the R foil exhibits a significantly lower level of creep (than does the ED foil). Except for the low temperature/low stress condition, the power law lines are roughly parallel with changing temperature or stress level. The R foil initially displays an exceptionally low level of creep at low (<1) σ/σ_y , but the extent of creep increases rapidly with time. Figures 5 and 6 show creep curves for the 18 and 12 μm ED foils, respectively. The effect of electrodeposit thickness on creep is illustrated in Fig. 7 for approximately equivalent σ and σ/σ_y . Again, decreasing foil thickness tends to shift the creep curve to a higher level and the thickness effect is greater at higher temperature, as was true for the stress relaxation (see Fig. 3).

The rolled foils were able to sustain very low strain prior to fracture; they also showed an anisotropy of deformation response along and across the rolling direction, consistent with the large cold reduction they had received and the ensuing pancaked grain structure. At 323K, embrittlement set in and the already low propensity to deform was further reduced. Within the temperature and time framework utilized in this study, the stress level below the yield stress, $(0.8-1.0) \sigma_y$, had no noticeable effect on the extent of creep strain; for $\sigma > \sigma_y$, the specimen ruptured during creep prior to the full 1800 s. Further, in spite of the grain size anisotropy, the creep strain vs time profile was roughly identical along and cross the rolling direction. These effects became more pronounced as the foil thickness decreased from 35 to 12 μm . Figure 8 compares the creep curves for the 12, 18, and 35 μm ED and R foils at 296, 323, and 348K for the identical creep stress or for $\sigma/\sigma_y = 1$. Not unexpectedly, for the R foil, no clear effect of foil thickness on creep can be demonstrated (compare thickness effect for the ED foil in Fig. 7). The creep curve for the ED foil is consistently higher than that for the R foil; this effect is enhanced (i) due to embrittlement, as at 323K whereby the ED and R creep curves are not parallel, and (ii) at high creep temperature, compare ED and R difference for the 35 μm foil at 296 and 348K.

DISCUSSION

Three facts emerge concerning the stress relaxation and creep of electrodeposit near yield stress and at or slightly above room temperature:

- (i) The logarithmic time law not obeyed,
- (ii) Significantly higher levels for the electrodeposit than for the rolled foil of same thickness, and
- (iii) Enhancement by decreasing electrodeposit thickness.

The distinguishing microstructural aspects of the electrodeposit are very fine, recovery prone grain structure and endemic atomic level microporosity;⁹ by comparison, the rolled foil has coarser, though anisotropic, grain structure and little or no microporosity. The deposit microporosity decreases gradually from the substrate side to the free surface.¹⁶ This gradation is apparently related to insufficient nucleation on the cathode surface and the formation of microvoids between the growth clusters.^{9,16} While the grain boundary sliding may play some role in items (i) to (iii) cited above, the microporosity appears to be the principal factor. The thickness effect for the normalized stress relaxation is sufficiently explicit (Fig. 3); that for the creep (Fig. 7) is hidden in part by fact that the yield strength changes with thickness (thinner deposit has higher strength). However, for equivalent σ/σ_y , a clear effect of deposit thickness on creep emerges. For $(\sigma/\sigma_y) < 1$, the thickness effect is not evident; for $(\sigma/\sigma_y) > 1$, it increases with σ/σ_y and with temperature. It is not surprising that the thickness effect is not observed for the rolled foil, since the heavy hot rolling prior to cold reduction may tend to decrease or eliminate any vestiges of casting microporosity. Its greater resis-

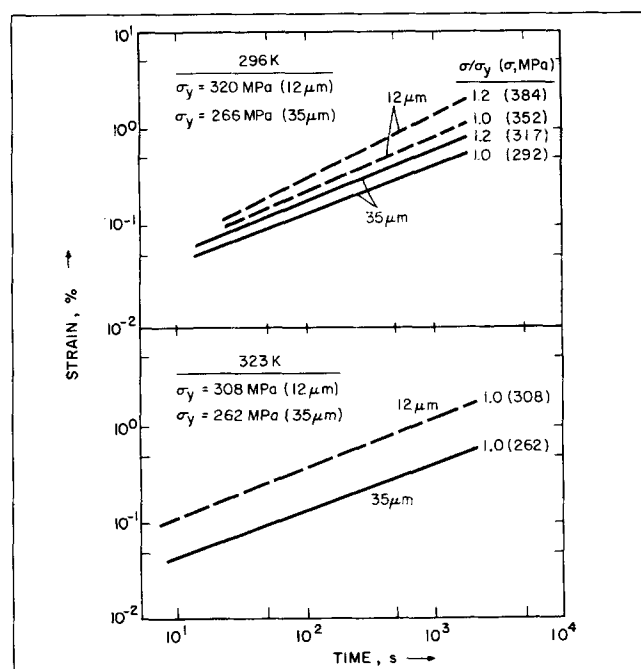


Fig. 7. Effect of ED foil thickness on creep.

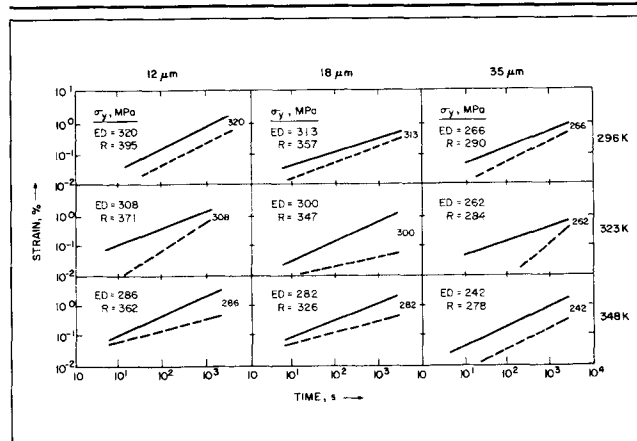


Fig. 8. A comparison of creep for ED (—) and R (---) foils at and near yield stress.

tance to creep and stress relaxation near room temperature and yield stress is apparently due to (a) lack of microporosity and (b) low temperature embrittlement and stiffening which typically occur in the ETP copper.¹⁷

CONCLUSIONS

Creep and stress relaxation of electrodeposits near yield stress and near room temperature do not follow the expected logarithmic variation with time; a power time law fits the data more accurately. The rolled foil displays significantly lower relaxation and creep (than does the electrodeposited foil). Decreasing the electrodeposit thickness from 35 to 12 μm enhances relaxation as well as creep. This effect increases as the relaxation or creep temperature is increased from 296 to 348K. The rolled foil does not display this thickness effect but is prone to embrittlement and stiffening at about 323K.

ACKNOWLEDGMENTS

The 12 μm rolled foil was provided by Dr. J. Miyake, Nippon Mining and Metals, Kanagawa, Japan. The stress relaxation and creep experiments were conducted by M. Minor; the TEM characterizations by S.K. Chiang (Gould) and F. Wong (University of Kentucky, Lexington).

REFERENCES

1. A. Fox, *J. Testing Evaluation* 4, 74 (1976).
2. L.A. Tumanova and T.D. Shermergor, *Phys. Met. Metall.* 34 (4), 207 (1972).
3. L.A. Tumanova and T.D. Shermergor, *Phys. Met. Metall.* 48 (3), 172 (1979).
4. I.T. Aleksanyan, *Phys. Met. Metall.* 25 (5), 189 (1968).
5. V.I. Verbkina, K.K. Ziling and L.D. Pokrovskiy, *Phys. Met. Metall.* 39 (5), 1086 (1975).
6. L.S. Palatnik and A.I. Il'inskii, *Sov. Phys. Usp.* 11, 564 (1969).
7. F.R. Brotzen, *Inter. Mater. Rev.* 39, 24 (1994).
8. A.I. Il'inskii, L.S. Palatnik and N.P. Sapelkin, *Sov. Phys. Solid State* 15, 2134 (1974).
9. H.D. Merchant, *Defect Structure, Morphology and Properties of Deposits*, ed. Harish D. Merchant, (Warrendale, PA: TMS, 1995), p. 1.
10. M.Y. Fuks, L.S. Palatnik, A.I. Il'inskii and V.V. Belozarov, *Sov. Phys. Solid State* 9, 588 (1967).
11. K.K. Ziling and V.Y. Pchelkin, *Zh. Prikl. Mekh. Tekh. Fiz.* (3), 442 (1970).
12. I.I. Solonovich, *Phys. Met. Metall.* 40 (3), 158 (1975).
13. F.R. Brotzen, C.T. Rosenmayer, C.G. Cofer and R.J. Gale, *Vacuum* 41, 1287 (1990).
14. R.J. DeAngelis, D.B. Knorr and H.D. Merchant, *J. Electron. Mater.* 24, 927 (1995).
15. H.D. Merchant, *J. Electron. Mater.* 22, 631 (1993).
16. T.R. Bergstresser and H.D. Merchant, *Defect Structure, Morphology and Properties of Deposits*, ed. Harish D. Merchant, (Warrendale, PA: TMS, 1995), p. 115.
17. T.G. Nieh and W.D. Nix, *Metall. Trans. A* 12A, 893 (1981).